

# Rhodamine-Based $\text{Cu}^{2+}$ -Selective Fluorosensor: Synthesis, Mechanism, and Application in Living Cells

Anindita Sikdar · Swapnadip Roy · Kakali Haldar · Soma Sarkar · Sujit S. Panja

Received: 4 October 2012 / Accepted: 31 January 2013 / Published online: 10 February 2013  
© Springer Science+Business Media New York 2013

**Abstract** A rhodamine B-based fluorescence probe (**1**) for the sensitive and selective detection of  $\text{Cu}^{2+}$  ion has been designed and synthesized using pyridine moiety. The optical properties of this compound have been investigated in acetonitrile-water binary solution (7:3 v/v). Compound **1** is found to be an excellent sensor for a biologically/physiologically very important transition metal ion ( $\text{Cu}^{2+}$ ) using only the two very different modes of measurements (absorption and emission); one case displayed intensity enhancement whereas in other case showed intensity depletion (quenching). A mechanistic investigation has been performed to explore the static nature of quenching process. The sensor has been found to be very effective in sensing  $\text{Cu}^{2+}$  ion inside living cells also.

**Keywords** Chemosensors · Rhodamine B · Cations · Static quenching · Living cells

## Introduction

The development of artificial chemosensors for selective and sensitive recognition of biologically and environmentally important ion species, especially transition-metal ions, has attracted wide-spread interests of chemists, biologists,

clinical biochemists and environmentalists in recent years [1–4]. Because of their many advantages e.g. low cost, simple instrumentation, high sensitivity and easy analysis, many efficient colorimetric/fluorescent sensors for transition-metal ions have been developed during the last two decades [1–8]. Generally, a typical synthesized probe of this type is constructed by covalent linkage of three parts: a chelating unit, a spacer and a reporting group, though there are some examples of spacer-free probes. Upon the binding of metal ions, these sensor molecules display completely different absorption/fluorescence signals compared to free sensors in solution, enabling the qualitative/quantitative determination of metal ions [9]. On the other hand, among the transition-metal ions of interest, divalent copper,  $\text{Cu}^{2+}$ , is particularly attractive, because it is not only an environmental pollutant at high concentrations [10, 11], but also an essential trace element for many biological processes and systems [12, 13]. Therefore, many excellent works of  $\text{Cu}^{2+}$  sensing colorimetric/fluorescent probes have been reported and investigated [14–19]. However, there is still an intense demand for new efficient  $\text{Cu}^{2+}$  optical chemosensors, especially those that can work in aqueous solution as well as in physiological condition with high selectivity and sensitivity [20–22]. Works related to this area are of great challenge and increasing interest and in the last half a decade there is almost a flood of different kinds of chemo/fluorosensors.

Rhodamines are classic dyes/fluorophores whose photochemical properties have already been well studied. Because of their low cost, long-wavelength absorption/emission and high molar absorption coefficient/quantum yield, these dyes/fluorophores are usually utilized as reporting groups in routine optical analysis. Since the work of Dujols' on the development of a highly selective and sensitive  $\text{Cu}^{2+}$  chemodosimeter derived from rhodamine B [23], many rhodamine derivatives have been designed and applied as efficient chemosensors for transition-metal ions [24–26]. These

**Electronic supplementary material** The online version of this article (doi:10.1007/s10895-013-1169-y) contains supplementary material, which is available to authorized users.

A. Sikdar · S. Roy · S. Sarkar · S. S. Panja (✉)  
Department of Chemistry, National Institute of Technology,  
Durgapur, W.B, India 713209  
e-mail: sujit.panja@gmail.com

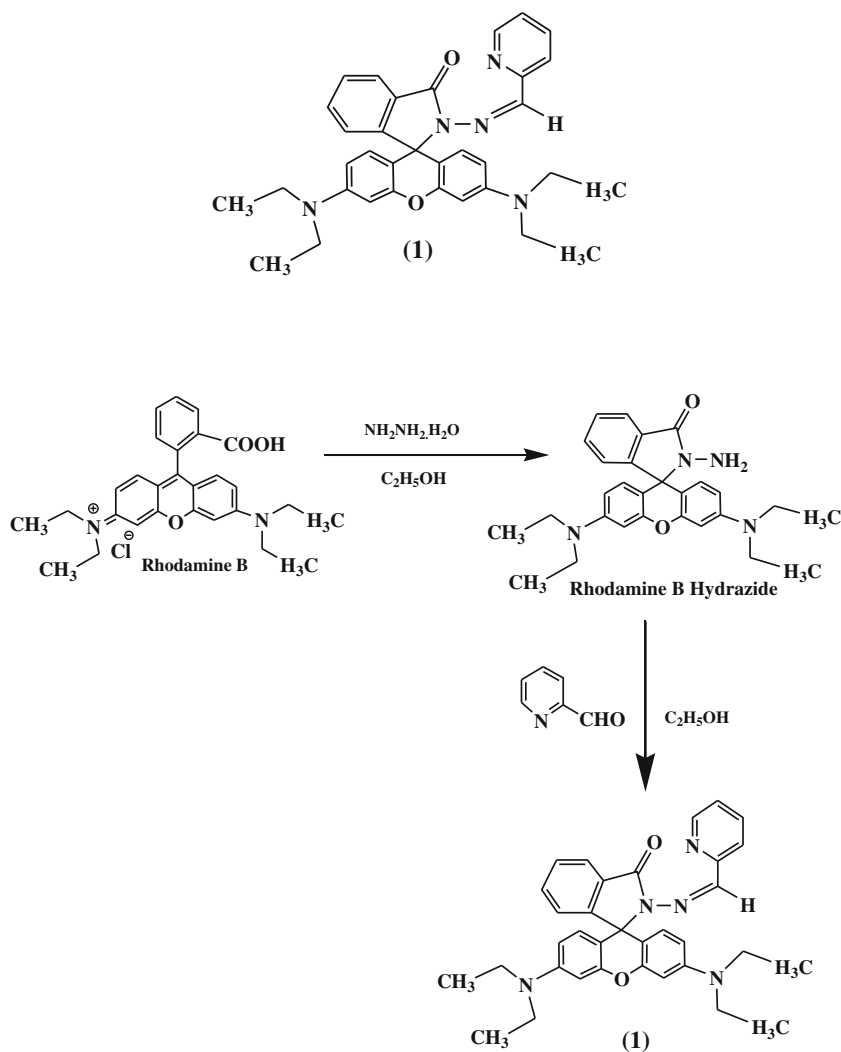
K. Haldar  
Department of Chemistry, MUC Women's College, Burdwan,  
W.B, India 713104

rhodamine-based ionophores not only exhibit the advantages of rhodamine dyes, but also display selective optical response to a specific metal ion after appropriate chemical modification. The metal ion sensing behaviour of these rhodamine-based optical sensors is very interesting. Typically, in the absence of metal ions, the sensor molecules prefer their spiro lactam ring-closed state, which shows no or little absorption or fluorescence in visible range (400–700 nm). However, upon the addition of specific cations (including protons), the chelating or reaction of metal ions with sensor molecules simultaneously open the spiro lactam ring and make the sensors converted into their ring-opened state [27], which becomes absorbent and fluorescent above 500 nm. So the effect of pH of the medium must be taken care of when rhodamines are used as sensor. Most of the reported rhodamine-based chemosensors for metal ions are of colorigenic or fluorogenic type. Nevertheless, there is still only a little study focused on the reversible detection of  $\text{Cu}^{2+}$  in aqueous solution using rhodamine derivatives [28, 29]. Reversible binding nature of the sensor towards selective metal ions may find its application in

different fields, e.g. efficient extraction of selective metal ions from an unknown gathering of metal ions.

The goal of this article is to report a rhodamine B-based Schiff base (**1**) which displayed excellent chemosensor characteristic for  $\text{Cu}^{2+}$  cation. From the absorption study it showed nice sensitivity and selectivity by signal enhancement and from emission study it responded through significant fluorescence quenching. We studied the mechanistic nature of the quenching behaviour of the compound on interaction with  $\text{Cu}^{2+}$  ion. Since the fluorescence technique offers significant advantages over other methods for metal ion monitoring inside living cells because of its non-destructive character, high sensitivity and instantaneous response, fluorescent probes for real-time sensing of biologically important ions and fluorescence imaging have become indispensable tools in numerous fields of modern medicine and science. We have also successfully applied our newly synthesized sensor to detect  $\text{Cu}^{2+}$  ion in living cell. The newly synthesized rhodamine-B derivative (**1**) was prepared in high yield as shown in Fig 1.

**Fig 1** Structure and Synthetic route of probe **1**



## Experimental

### General Methods

Solvents and reagents were purchased from Aldrich and used as received. The solvents for spectroscopic studies were of HPLC grade and used as received. All the metal ions used are mainly of nitrates, chlorides, perchlorates or sulphates.  $^1\text{H}$  NMR spectrum of the ligand, **1** was recorded on JEOL ECX-500. Mass spectrum was recorded under ESI mode on a Micromass Q-TOF micro<sup>TM</sup> instrument. The Fourier transform infrared spectrum of the ligand (**1**) and the  $\text{Cu}^{2+}$  complex were recorded on a ThermoNicolet iS10 spectrophotometer using KBr pellet in the range of 4,000–400  $\text{cm}^{-1}$ . UV–vis spectra were measured on a Simadzu UV-1800 spectrophotometer and fluorescence spectra were recorded using a Hitachi F-2500 spectrofluorimeter. The solution was allowed to stand for 5 min at room temperature (30 °C) before an absorption/fluorescence measurement was made. The intensity of the fluorescence was measured at 578 nm ( $\lambda_{\text{ex}}=520$  nm) in a 1 cm quartz cell with a slit width of 5 nm for both excitation and emission path.

### Fluorescence Imaging

A single colony of E-coli was inoculated over-night in 10 ml of LB-medium at 37°C temp. After that it was centrifuged at 3,000 rpm for 10 min, washed twice with 0.1(M) Tris–HCl buffer containing  $\text{CH}_3\text{CN}/\text{H}_2\text{O}$  (7:3,v/v) (pH-7) solution. Cells were then treated with different concentrations of  $\text{Cu}^{2+}$  (100  $\mu\text{M}$ , 500 $\mu\text{M}$  resp.) for 30 min in 0.1(M) Tris–HCl buffer (pH-7.04) containing 0.01 % Triton X100 as permeability enhancing agent. After incubation, cells were washed with 0.1(M) Tris–HCl buffer (pH-7) and incubated with probe **1** (10  $\mu\text{M}$ ) for 30 min. Cells obtained were mounted on grease free glass slides and observed under the Fluorescence Microscope equipped with UV filter. Cells incubated with  $\text{Cu}^{2+}$  were used as control. Both cells ( $\text{Cu}^{2+}$  treated and untreated) were stained with probe **1** and observed under the Fluorescence Microscope (DE—Winter Premium Fluorescence Imaging).

### Synthetic Procedure

To synthesis rhodamine B hydrazide, in a 100 mL flask, rhodamine B (1.20 g, 2.5 mmol) was dissolved in 30 mL ethanol. 12.5 mL (excess) hydrazine hydrate (24 %) was then added drop wise with vigorous stirring at room temperature. After the addition, the stirred mixture was heated to reflux in an air bath for 4–5 h. The solution changed from dark pink to light orange. Then the mixture was cooled and solvent was removed under reduced pressure. 1 M HCl(50 mL) was added to the solid in the flask to generate

a clear red solution. After that, 1 M NaOH(70 mL) was added slowly with stirring until the pH of the solution reached 9–10. The resulting precipitate was filtered and washed 3 times with 15 mL water. After drying under an IR light, the reaction afforded 0.93 g rhodamine B hydrazide (81.3 %) as pink solid.

For the preparation of compound **1**, rhodamine B hydrazide (0.46 g, 1 mmol) was dissolved in 20 mL absolute ethanol. An excess of aldehyde (pyridine-2-aldehyde) (4 mmol) was added and then the mixture was refluxed in an air bath for 7–8 h. After that, the solution was cooled (reduced to 10 mL) and allowed to stand at room temperature overnight. The precipitate which appeared next day was filtered and washed 3–4 times with 10 mL of cold ethanol. After drying under reduced pressure, the reaction afforded 0.38 g of **1** (70.35 %) as dirty white solid. The resulting solid was further purified by column chromatography.  $^1\text{H}$  NMR (500 MHz,  $\text{CDCl}_3$ )

$\delta$  (ppm): 8.46–8.45 (bd, 1H, Py-H), 8.34 (s, 1H, Imine-H), 8.01–7.99 (m, 2H, Py-H (1), Ar-H (1)), 7.6 (t, 1H, Py-H), 7.48–7.43 (m, 2H, Ar-H), 7.13–7.09 (m, 2H, Py-H(1), Ar-H(1)), 6.54–6.53 (d, 2H, Xanthene-H), 6.44 (d, 2H, Xanthene-H), 6.23–6.21 (dd, 2H, Xanthene-H), 3.32–3.28 (q, 8H,  $\text{NCH}_2\text{CH}_3$ ), 1.15–1.12 (t, 12H,  $\text{NCH}_2\text{CH}_3$ ) as shown in figure (Fig.S1, ESI). ESI-MS mass spectra of **1** exhibited peak at ( $m/z=546.30$ ), ( $m/z=547.31$ ) and ( $m/z=569.29$ ) which corresponds to [1], [**1**+H]<sup>+</sup> and [**1**+Na]<sup>+</sup> respectively (Fig. S2, ESI).

## Results and Discussion

Here we report a rhodamine B-based Schiff base as colorimetric/fluorimetric sensor for a physiologically and environmentally very important metal ion,  $\text{Cu}^{2+}$ . The Fig. 2a shows the absorption spectra of **1** in Tris–HCl buffer containing  $\text{CH}_3\text{CN}/\text{H}_2\text{O}$  (7:3 v/v) solution at pH7 in presence of different metal ions. It is seen that there is no absorption for **1** after 450 nm wavelength suggesting that the spiro-lactam ring of rhodamine B unit preferred its ring-closed state at this condition. The same observation prevails when different metal and non-metal cations (e.g.  $\text{Co}^{2+}$ ,  $\text{Ni}^{2+}$ ,  $\text{Hg}^{2+}$ ,  $\text{Mn}^{2+}$ ,  $\text{Pb}^{2+}$ ,  $\text{Zn}^{2+}$ ,  $\text{Cd}^{2+}$ ,  $\text{Cr}^{3+}$ ,  $\text{Fe}^{3+}$ ,  $\text{Fe}^{2+}$ ,  $\text{Mg}^{2+}$ ,  $\text{Ca}^{2+}$ ,  $\text{Ba}^{2+}$ ,  $\text{Li}^+$ ,  $\text{Na}^+$ ,  $\text{K}^+$ ,  $\text{NH}_4^+$  and  $\text{Ag}^+$ ) are added to the solution of **1**. However, there is only a remarkable enhancement of absorption in the range of 475–600 nm upon addition of  $\text{Cu}^{2+}$  as chloride salt to the solution of **1**. We found a significant absorption at 558 nm along with a shoulder at 522 nm. The absorbance increased gradually with increasing  $\text{Cu}^{2+}$  concentration and the solution turned pink from colorless instantaneously. At this point it must be mentioned that although  $\text{Co}^{2+}$  ion shows a very weak and red-shifted response but can be ignored as evident from the figure. The

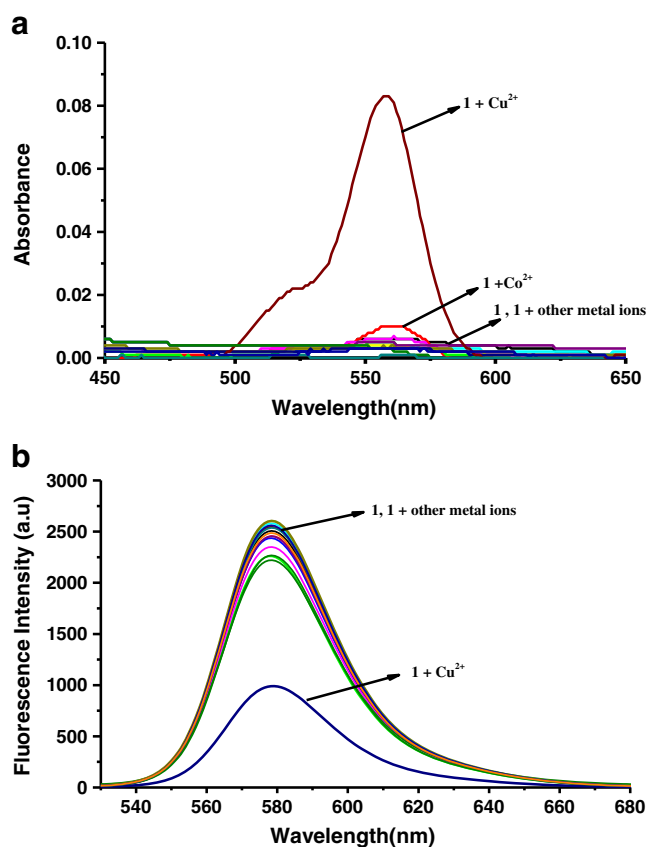


**Fig 2** Changes in the (a) absorption spectra (at pH7) and (b) fluorescence spectra (at pH3) of **1** ( $5.0 \times 10^{-6}$  M) in the presence of various metal ions ( $\text{Co}^{2+}$ ,  $\text{Ni}^{2+}$ ,  $\text{Cu}^{2+}$ ,  $\text{Hg}^{2+}$ ,  $\text{Mn}^{2+}$ ,  $\text{Pb}^{2+}$ ,  $\text{Zn}^{2+}$ ,  $\text{Cd}^{2+}$ ,  $\text{Cr}^{3+}$ ,  $\text{Fe}^{3+}$ ,  $\text{Fe}^{2+}$ ,  $\text{Mg}^{2+}$ ,  $\text{Ca}^{2+}$ ,  $\text{Ba}^{2+}$ ,  $\text{Li}^{+}$ ,  $\text{Na}^{+}$ ,  $\text{K}^{+}$ ,  $\text{NH}_4^{+}$ ,  $\text{Ag}^{+}$ ) of concentration  $2.0 \times 10^{-4}$  M in Tris-HCl (10 mM, pH = 7) buffer containing (7:3 v/v)  $\text{CH}_3\text{CN}/\text{H}_2\text{O}$

absorption band appeared was the characteristic absorption pattern of rhodamine B (542 nm). Thus it could be inferred that due to the formation of a ground state complex between **1** and  $\text{Cu}^{2+}$  through the oxygen atom of the amide moiety of (**1**) the spirolactam ring of rhodamine B unit is opened up. This, in turn, shows intense absorption because of the formation of a highly delocalized  $\pi$ -conjugated stable complex through their active donor sites (viz. amide O, pyridine N and imino N atoms) of the receptor part, although other ions failed which basically indicates that the coordinate moiety of **1** matches perfectly with  $\text{Cu}^{2+}$  ion instead of the other ions.

The high absorption may be attributed to highly crowded and asymmetric nature around the  $\text{Cu}^{2+}$  ion which results in an increase of transition dipole moment and hence oscillator strength. The absorption titration curve has been shown in (Fig. S3, ESI) and found that after addition of about 80 equivalent of  $\text{Cu}^{2+}$  ion, the intensity gets saturated (Inset). Further it is seen that in absence of  $\text{Cu}^{2+}$  ion the probe **1** shows weak absorption only in the range of pH2–5 (Fig. S4a, ESI). This may be attributed to small degree of  $\text{H}^{+}$  ion-

assisted spirolactam ring opening at lower pH. In presence of  $\text{Cu}^{2+}$  ion an appreciable absorbance is found through a pH range of ~2 to 8 due to predominant  $\text{Cu}^{2+}$  ion –assisted ring opening of rhodamine. All the absorption studies have been chosen at ~pH7 which is a physiologically important pH too.

To get into the further insight, the fluorescence responses of chemosensor **1** towards  $\text{Cu}^{2+}$  and other metal ions were investigated and shown in Fig. 2b. It is found that the free **1** in  $\text{CH}_3\text{CN}/\text{H}_2\text{O}$  (7:3) binary solution displayed a band centred at 578 nm in the emission spectra. This observation is quite different from most of the reported rhodamine-based chemosensors with no obvious fluorescence signal before the complexation with some specific metal ions due to the existence of predominant spirocyclic form. In the present study, while in presence of  $\text{Cu}^{2+}$  there is a clear increase in the intensity of the absorption spectrum, the fluorescence was significantly quenched in stark contrast to other metal ions, where no significant fluorescence changes were observed. Even with highly concentrated solution of metal ions (except  $\text{Cu}^{2+}$ ) could hardly make any changes in the fluorescence intensity. This may be attributed to  $\text{Cu}^{2+}$ -induced opening up of an additional non-radiative deactivation channel upon interaction of **1** with  $\text{Cu}^{2+}$ . From the Fig.S4b, ESI it is evident that above pH5 there was no appreciable fluorescence signal for **1** as well as **1**- $\text{Cu}^{2+}$  complex. Significant fluorescence is found in the pH range of 2 to 5 with a maximum at pH3. So to get significant fluorescence response pH3 was selected for all fluorescent assays. From the figure it is also evident that even in presence of a large number of  $\text{H}^{+}$  ion (at pH3) the  $\text{Cu}^{2+}$  ion can restore its sensitivity through formation of a stable complex with **1** and subsequent quenching of fluorescence signal. So it can be concluded that, although there is a small effect due to  $\text{H}^{+}$  ion,  $\text{Cu}^{2+}$  ion is a better competitor as compared to  $\text{H}^{+}$  ion as far as the spirolactam ring opening is concerned. The pH study of absorption and fluorescence for sensor is very important as there are several examples of switch over of selectivity depending upon the pH of the medium [30–32].

In order to make sure that these selective changes in absorption and fluorescence of compound **1** were entirely due to only the presence of  $\text{Cu}^{2+}$  ion, the effects of different anions of copper salts (e.g. acetate, chloride, sulphate and nitrate) were also tested. There were no obvious changes in the absorption and fluorescence responses of compound **1** to  $\text{Cu}(\text{AcO})_2$ ,  $\text{CuCl}_2$ ,  $\text{Cu}(\text{SO}_4)_2$  and  $\text{Cu}(\text{NO}_3)_2$  salts.

By measuring the emission maximum of **1**- $\text{Cu}^{2+}$  complex, the fluorescence change of **1** responds to the range of 0–140 equivalent of  $[\text{Cu}^{2+}]$  which is shown in Fig. S5, ESI. From the titration data we found that **1** shows  $1.22 \mu\text{M}$  of detection limit able to sufficiently sense the  $\text{Cu}^{2+}$  concentration in a system. Moreover, this detection limit is very much satisfactory to the  $\text{Cu}^{2+}$  detection in drinking water within U.S. EPA limit ( $\sim 20 \mu\text{M}$ ).

It is well known that rhodamine-based chemosensors always show a fluorescence enhancement response (turn on) upon the addition of analytes. As far as our knowledge, only a very few articles are there which reported the fluorescence depletion after addition of foreign analytes [33, 34]. The fluorescence quenching of the probe may be explained by the paramagnetic nature of  $\text{Cu}^{2+}$  ion ( $d^9$  system) which easily participates in the excitation energy transfer from the ligand to metal d-orbital and/or ligand to metal charge transfer [35, 36] by opening a non-radiative deactivation channel. While the quantum yield of pure **1** was found to be 0.21 (Rhodamine B was used as standard), the quantum yield of **1**- $\text{Cu}^{2+}$  complex was calculated as 0.02. These results indicated a substantial quenching of fluorescence of **1** in presence of  $\text{Cu}^{2+}$ .

To get an insight into the quenching behaviour in **1**- $\text{Cu}^{2+}$  complex, we measured the fluorescence intensity in absence and presence of increasing concentrations of quencher  $\text{Cu}^{2+}$  ion. The Stern-Volmer plot for **1**- $\text{Cu}^{2+}$  complex using the simple model of static quenching  $F_0/F = 1 + K_{sv}[Q]$  showed a linear fit ( $F_0$  stands for emission intensity in absence of  $\text{Cu}^{2+}$  ion,  $F$  indicates intensity after addition of  $\text{Cu}^{2+}$  ion,  $[Q]$  is the quencher concentration and  $K_{sv}$  is the static Stern-Volmer constant). Assuming that the quenching process is following static mechanism, we calculated the association constant ( $K_{sv}$ ) for the **1**- $\text{Cu}^{2+}$  complex and found to be  $1.2 \times 10^4$  at 30 °C temperature. Now since both static and dynamic quenching gives a linear Stern-Volmer plot, it cannot be reached to any unambiguous decision about the mechanism of the quenching. Those mechanisms can be clearly distinguished from each other by their differing dependence on temperature. From the Stern-Volmer plot at two different temperatures (Fig. 3) it was found that with increase in

temperature, the slope of the curve and hence the magnitude of association constant ( $K_{sv} = 4.09 \times 10^3$  at 50 °C) decreased. There was almost a ten-fold decrease in  $K_{sv}$  with 20 °C rise in temperature. This observation is in good agreement with static quenching mechanism as with increased temperature is likely to result in decreased stability of the **1**- $\text{Cu}^{2+}$  complex in the ground state and thus lowers the value of static quenching constant ( $K_{sv}$ ). This static quenching mechanism has been nicely described (Inset Fig. 3), where it is seen that due to formation of weak/non-fluorescent **1**- $\text{Cu}^{2+}$  complex less number of **1** molecules left over for excitation and hence subsequent manifestation of lower degree of fluorescence. Another way of supporting the above quenching mechanism is by careful examination of absorption spectra of the fluorophore. Since static quenching is a phenomena of ground state complex formation, it will result in perturbation of the absorption spectra of the fluorophore, whereas, dynamic quenching only affects the excited states of fluorophores and thus no change in the absorption spectra are predicted. Here we see some perturbation in the absorption spectra of **1** after complexation with  $\text{Cu}^{2+}$  ion (Fig. S6, ESI). To establish the selectivity of **1** toward  $\text{Cu}^{2+}$  over a range of various metallic and non-metallic cations ( $\text{Li}^+$ ,  $\text{Na}^+$ ,  $\text{K}^+$ ,  $\text{Mg}^{2+}$ ,  $\text{Ca}^{2+}$ ,  $\text{Mn}^{2+}$ ,  $\text{Co}^{2+}$ ,  $\text{Fe}^{2+}$ ,  $\text{Fe}^{3+}$ ,  $\text{Ni}^{2+}$ ,  $\text{Ag}^+$ ,  $\text{Zn}^{2+}$ ,  $\text{Cd}^{2+}$ ,  $\text{Ba}^{2+}$ ,  $\text{Hg}^{2+}$ ,  $\text{NH}_4^+$  and  $\text{Pb}^{2+}$ ), we carried out the competitive recognition studies where the other cations were used even in higher concentrations (Fig. S7, ESI). From the bar diagram, the negligibly small effect of various cations on absorption and fluorescence measurements were evident. Therefore, it was clear that other ions' interference, even in higher concentrations, was negligibly small during the detection of  $\text{Cu}^{2+}$ . These results further suggested that **1** could be used as an effective two way sensor through absorption 'on' and fluorescence 'off' transduction for  $\text{Cu}^{2+}$  over a wide range of metallic and non-metallic cations.

Meanwhile, we have measured the absorption spectra with a number of different solvents in which the compound (**1**) is appreciably soluble. The figure (Fig. S8, ESI) shows that among the different solvents, in acetonitrile-water binary solvent maximum absorbance was obtained indicating that acetonitrile-water solution is favourable for colorimetric assay. The effect of acetonitrile content on the absorption and fluorescence measurements of **1**- $\text{Cu}^{2+}$  complex was investigated and the results were shown in Fig. S9, ESI. It can be observed that for both absorption and fluorescence at 70 % aqueous acetonitrile an appreciable and stable signal was obtained. Therefore, 70 % aqueous acetonitrile solution was chosen for all subsequent experiments.

Binding analysis using the method of continuous variations (Job's plot) established that the estimated stoichiometry of the **1**- $\text{Cu}^{2+}$  complex is 1:1 (Fig. S10, ESI), since the maximum absorbance (i.e. maximum complex formation) was found when the mole fraction of  $\text{Cu}^{2+}$  ion added was

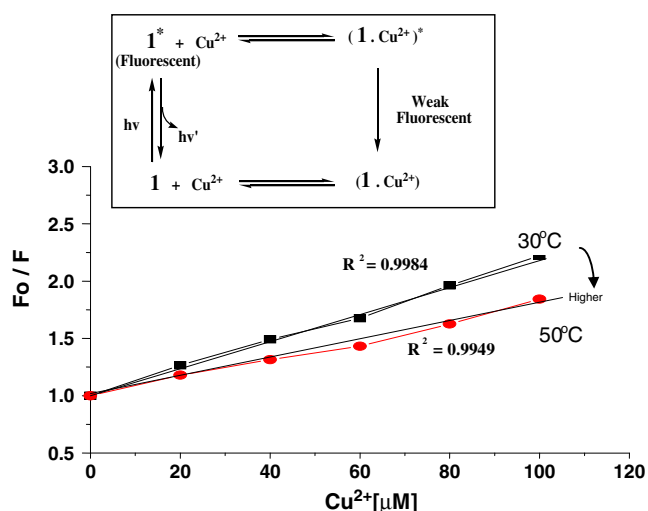


**Fig 3** Stern-Volmer plot of **1** in the presence of  $\text{Cu}^{2+}$  at room (30 °C) and higher (50 °C) temperature. *Inset*: Mechanism of static quenching of **1** by  $\text{Cu}^{2+}$

50 %. For further confirmation of the stoichiometry of the **1**-Cu<sup>2+</sup> complex we generated Benesi-Hildebrand Plot (Fig. S11, ESI) from the absorption titration data and from the plot the calculated binding constant was estimated to be  $2.5 \times 10^4$  which is in good agreement with the result obtained previously.

Further, it was of great interest to investigate the reversible binding nature of the sensor which finds its new applicability from the view point of chemistry (e.g., extraction of a particular analyte from a mixture of different analytes) when it shows reversible binding nature. Upon gradual addition of CH<sub>3</sub>CN/H<sub>2</sub>O (7:3) solution of KI to a solution mixture of **1** (10 μM) and Cu(II) (200 μM), color changed slowly from pink to colorless. This observation is assumed to be due to decomplexation of Cu(II) by I<sup>-</sup> followed by a spirolactam ring closure reaction. Thus, **1** can be used as a reversible chemosensor for Cu<sup>2+</sup>. Similar observation was also found during the fluorescence measurement shown in (Fig. S12, ESI) where fluorescence intensity was fully recovered after addition of excess KI.

Meanwhile, IR spectra of **1** and **1**-Cu<sup>2+</sup> complex were recorded in KBr disks (Fig. S13, ESI) and part of the results has been shown in Fig. 4. The peak at 1,723 cm<sup>-1</sup>, which corresponds to the characteristic amide carbonyl absorption of **1**, was shifted to a lower value of 1,647 cm<sup>-1</sup> upon chelating with Cu<sup>2+</sup>. Similarly, the imine C=N frequency decreases from 1,617 cm<sup>-1</sup> to 1,589 cm<sup>-1</sup> and pyridine ring C=N frequency decreases from 1,547 cm<sup>-1</sup> to 1,528 cm<sup>-1</sup> after complexation with Cu<sup>2+</sup> ion. These results indicate that carbonyl O-atom, imine N-atom and pyridine N-atom are surely involved in Cu<sup>2+</sup> coordination as we have mentioned earlier in this paper.

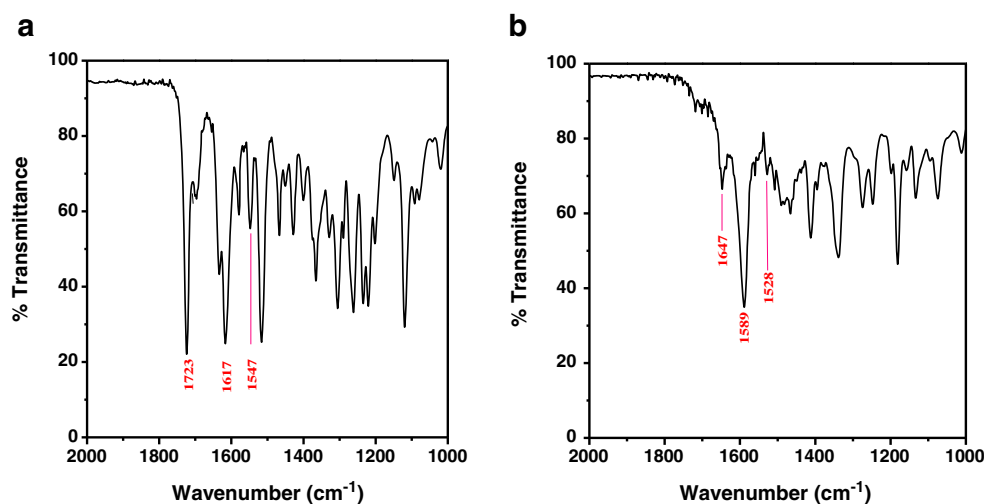
The ability of the sensor molecules to selectively monitor guest species in living cells is of great importance for biological application [37, 38]. In this regard, we tried to detect Cu<sup>2+</sup> ion present inside a living cell using our

newly synthesized sensor. Considering that copper accumulation leads to toxicity in animals, we primarily carried out experiment using **1** on living cell e.g. E-coli cell in which Cu<sup>2+</sup> was accumulated from external source after increasing the permeability of the cell membrane using 0.01 % Titron X100. The results are shown in Fig. S14, ESI and one can clearly observe significant confocal imaging changes of the medium upon addition of Cu<sup>2+</sup> for 15 min (0, 10 and 50 equiv, respectively) at 37 °C. Although all the fluorescence measurements were done at pH3 to get strong fluorescence, as also evident from pH study, the fluorescence imaging study has been tried at pH7 to have greater biological implication and indeed we got nice image at that pH. E-coli cells incubated with **1** initially displayed a strong fluorescent image (Fig. S14b, ESI), but the fluorescence image immediately becomes faint in the presence of increasing concentration of Cu<sup>2+</sup> which is evident from Fig. S14c,d, ESI.

## Conclusions

In summary, we have developed a rhodamine B-based chemosensor bearing xanthenes and pyridine group for the detection of biologically/physiologically very important transition metal ion, Cu<sup>2+</sup>. Chemosensor **1** displayed selective fluorescent and colorimetric changes upon addition of Cu<sup>2+</sup>. Compound **1** is found to be an excellent sensor for Cu<sup>2+</sup> using either of the two very modes of measurements (absorption and emission); one case displays intensity enhancement whereas in other case shows fluorescence depletion respectively. A mechanistic investigation has been performed to explore the nature of fluorescence quenching. The sensor has been applied efficiently in living cells to sense biologically and physiologically very important Cu<sup>2+</sup> ion.

**Fig. 4** IR Spectra of compound (a) **1** and (b) **1**-Cu<sup>2+</sup> complex in KBr disks



**Acknowledgments** This work was fully supported by DST, Govt. of India (No. SR/FT/CS-047/2008). The authors are also thankful to Dr. A. K. Patra and Dr. D. Sukul for fruitful discussion. We gratefully acknowledge the help of Dr. Anjil Srivastava and Minati Behra (Dept. of Biotechnology NIT Durgapur) for fluorescence image recording.

## References

- Wu J, Liu W, Ge J, Zhang H, Wang P (2011) New sensing mechanisms for design of fluorescent chemosensors emerging in recent years. *Chem Soc Rev* 40(7):3483–3495
- Lohani CR, Kim JM, Chung SY, Yoon J, Lee KH (2010) Colorimetric and fluorescent sensing of pyrophosphate in 100 % aqueous solution by a system comprised of rhodamine B compound and  $Al^{3+}$  complex. *Analyst* 135(8):2079–2084
- de Silva AP, Gunaratne HQN, Gunnlaugsson T, Huxley AJM, McCoy CP, Rademacher JT, Rice TE (1997) Signaling recognition events with fluorescent sensors and switches. *Chem Rev* 97(5):1515–1566
- Pu L (2004) Fluorescence of organic molecules in chiral recognition. *Chem Rev* 104(3):1687–1716
- Gokel GW, Leevy WM, Weber ME (2004) Crown ethers: sensors for ions and molecular scaffolds for materials and biological models. *Chem Rev* 104(5):2723–2750
- Sahana A, Banerjee A, Das S, Lohar S, Karak D, Sarkar B, Mukhopadhyay SK, Mukherjee AK, Das D (2011) A naphthalene-based  $Al^{3+}$  selective fluorescent sensor for living cell imaging. *Org Biomol Chem* 9(15):5523–5529
- Prodi L, Bolletta F, Montalti M, Zaccaroni N (2000) Luminescent chemosensors for transition metal ions. *Coord Chem Rev* 205(1):59–83
- Amendola V, Fabbrizzi L, Forti F, Licchelli M, Mangano C, Pallavicini P, Poggi A, Sacchi D, Taglietti A (2006) Light-emitting molecular devices based on transition metals. *Coord Chem Rev* 250(3–4):273–293
- Valeur B, Leray I (2000) Design principles of fluorescent molecular sensors for cation recognition. *Coord Chem Rev* 205(1):3–40
- High B, Bruce D, Richter MM (2001) Determining copper ions in water using electrochemiluminescence. *Anal Chim Acta* 449(1–2):17–22
- Tapia L, Suazo M, Hodar C, Cambiazo V, Gonzalez M (2003) Copper exposure modifies the content and distribution of trace metals in mammalian cultured cells. *Biometals* 16(1):169–174
- Sigel H (1981) Metal ions in biological systems, properties of copper, vol 12. Dekker, New York
- Waggoner DJ, Bartnikas TB, Gitlin JD (1999) The role of copper in neurodegenerative disease. *Neurobiol Dis* 6(4):221–230
- Krämer R (1998) Fluorescent chemosensors for  $Cu^{2+}$  ions: fast, selective, and highly sensitive. *Angew Chem Int Ed* 37(6):772–773
- Ghosh P, Bharadwaj PK, Mandal S, Sanjib G (1996)  $Ni(II)$ ,  $Cu(II)$ , and  $Zn(II)$  cryptate-enhanced fluorescence of a trianthrylcryptand: a potential molecular photonic OR operator. *J Am Chem Soc* 118(6):1553–1554
- Zheng Y, Orbulescu J, Ji X, Andreopoulos FM, Pham SM, Leblanc RM (2003) Development of fluorescent film sensors for the detection of divalent copper. *J Am Chem Soc* 125(9):2680–2686
- Royzen M, Dai Z, Canary JW (2005) Ratiometric displacement approach to  $Cu(II)$  sensing by fluorescence. *J Am Chem Soc* 127(6):1612–1613
- Sumner JP, Westerberg NM, Stoddard AK, Hurst TK, Cramer M, Thompson RB, Fierke CA, Kopelman R (2006) DsRed as a highly sensitive, selective, and reversible fluorescence-based biosensor for both  $Cu^+$  and  $Cu^{2+}$  ions. *Biosens Bioelectron* 21(7):1302–1308
- Yang H, Liu ZQ, Zhou ZG, Shi EX, Li FY, Du YK, Yi T, Huang CH (2006) Highly selective ratiometric fluorescent sensor for  $Cu(II)$  with two urea groups. *Tetrahedron Lett* 47(17):2911–2914
- Zheng Y, Cao X, Orbulescu J, Konka V, Andreopoulos FM, Pham SM, Leblanc RM (2003) Peptidyl fluorescent chemosensors for the detection of divalent copper. *Anal Chem* 75(7):1706–1712
- Mokhir A, Krämer R (2005) Double discrimination by binding and reactivity in fluorescent metal ion detection. *Chem Commun* 2244–2246
- Kovács J, Rödler T, Mokhir A (2006) Chemodosimeter for  $CuII$  detection based on cyclic peptide nucleic acids. *Angew Chem Int Ed* 45(46):7815–7817
- Dujols V, Ford F, Czarnik AW (1997) A long-wavelength fluorescent chemodosimeter selective for  $Cu(II)$  ion in water. *J Am Chem Soc* 119(31):7386–7387
- Yang YK, Yook KJ, Tae J (2005) A rhodamine-based fluorescent and colorimetric chemodosimeter for the rapid detection of  $Hg^{2+}$  ions in aqueous media. *J Am Chem Soc* 127(48):16760–16761
- Kwon JY, Jang YJ, Lee YJ, Kim KM, Seo MS, Nam W, Yoon J (2005) A highly selective fluorescent chemosensor for  $Pb^{2+}$ . *J Am Chem Soc* 127(28):10107–10111
- Xiang Y, Mei L, Li N, Tong A (2007) Sensitive and selective spectrofluorimetric determination of chromium(VI) in water by fluorescence enhancement. *Anal Chim Acta* 581(1):132–136
- Nguyen T, Francis MB (2003) Practical synthetic route to functionalized rhodamine dyes. *Org Lett* 5(18):3245–3248
- Xiang Y, Tong A, Jin P, Ju Y (2006) New fluorescent rhodamine hydrazone chemosensor for  $Cu(II)$  with high selectivity and sensitivity. *Org Lett* 8(13):2863–2866
- Sikdar A, Panja SS, Biswas P, Roy S (2012) A rhodamine-based dual chemosensor for  $Cu(II)$  and  $Fe(III)$ . *J Fluoresc* 22(1):443–450
- Sarkar M, Banthia S, Patil A, Ansari MB, Samanta A (2006) pH-Regulated “Off–On” fluorescence signalling of d-block metal ions in aqueous media and realization of molecular IMP logic function. *New J Chem* 30(11):1557–1560
- Yuan L, Lin W, Fung Y (2011) A rational approach to tuning the  $pK_a$  values of rhodamines for living cell fluorescence imaging. *Org Biomol Chem* 9(6):1723–1726
- Xiang Y, Li Z, Chen X, Tong A (2008) Highly sensitive and selective optical chemosensor for determination of  $Cu^{2+}$  in aqueous solution. *Talanta* 74(5):1148–1153
- Ding J, Yuan L, Gao L, Chen J (2012) Fluorescence quenching of a rhodamine derivative: selectively sensing  $Cu^{2+}$  in acidic aqueous media. *J Lumin* 132(8):1987–1993
- Jung HS, Kwon PS, Lee JW, Kim JI, Hong CS, Kim JW, Yan S, Lee JY, Lee JH, Joo T, Kim JS (2009) Coumarin-derived  $Cu^{2+}$ -selective fluorescence sensor: synthesis, mechanisms, and applications in living cells. *J Am Chem Soc* 131(5):2008–2012
- Ressalan S, Iyer CSP (2005) Absorption and fluorescence spectroscopy of 3-hydroxy-3-phenyl-1-*o*-carboxyphenyltriazene and its copper (II), nickel (II) and zinc (II) complexes: a novel fluorescence sensor. *J Lumin* 111(3):121–129
- Liu J, Li C, Li F (2011) Fluorescence turn-on chemodosimeter-functionalized mesoporous silica nanoparticles and their application in cell imaging. *J Mater Chem* 21(20):7175–7181
- Banerjee A, Sahana A, Das S, Lohar S, Guha S, Sarkar B, Mukhopadhyay SK, Mukherjee AK, Das D (2012) A naphthalene exciplex based  $Al^{3+}$  selective on-type fluorescent probe for living cells at the physiological pH range: experimental and computational studies. *Analyst* 137(9):2166–2175
- Liu WY, Li HY, Zhao BX, Miao JY (2012) A new fluorescent and colorimetric probe for  $Cu^{2+}$  in live cells. *Analyst* 137(15):3466–3469